Supplement of Nat. Hazards Earth Syst. Sci., 18, 647–668, 2018
https://doi.org/10.5194/nhess-18-647-2018-supplement

Natural Hazards and Earth System Sciences
Open Access
EGU

Supplement of

Sediment traps with guiding channel and hybrid check dams improve controlled sediment retention

Sebastian Schwindt et al.

Correspondence to: Sebastian Schwindt (sschwindt@ucdavis.edu)

1 Application of the motion sensing device

The comparison of V_{dep} (Scale) and V_{dep} (Bathymetric) was used to evaluate the percentaged error ε_v of the bathymetric tools (except for the case *Hy–no*, where sediment flushing was examined after the hydrograph).

$$\varepsilon_v = \left[V_{dep}(Bathymetric) - V_{dep}(Scale)\right] / V_{dep}(Scale) \cdot 100, \quad (2)$$

The error ε_v is shown in Figure 1 for the cases *Mec* and *HyMec*, where the bar screen was applied. The graphs show that both bathymetric techniques tend to underestimate the deposit, but this effect is significantly less pronounced for the sensor data (in average, ε_v = 2.7%) than for the laser data (in average, ε_v = 14.8%).

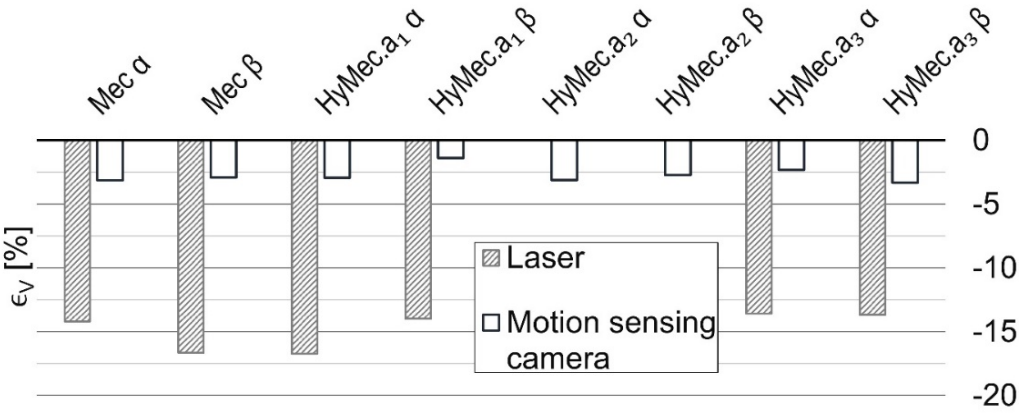

Figure 1: Percentage error ε_v of the sediment volume derived from weight measurements (assuming ρ_s' = 1 550 kg/m³) and the deposit volume measurements based on the bathymetric scans using the laser and the motion sensing device; the bathymetric records were made after the repetitive α and β tests with the bar screen only (*Mec*) and the combination of the bar screen with the open hydraulic barrier *HyMec*, with varying opening heights $a_{1,2,3}$.

Figure 2 shows an example application of the bathymetric recording of the deposit using the motion-sensing device after the test *HyMec.a*$_1$ α.

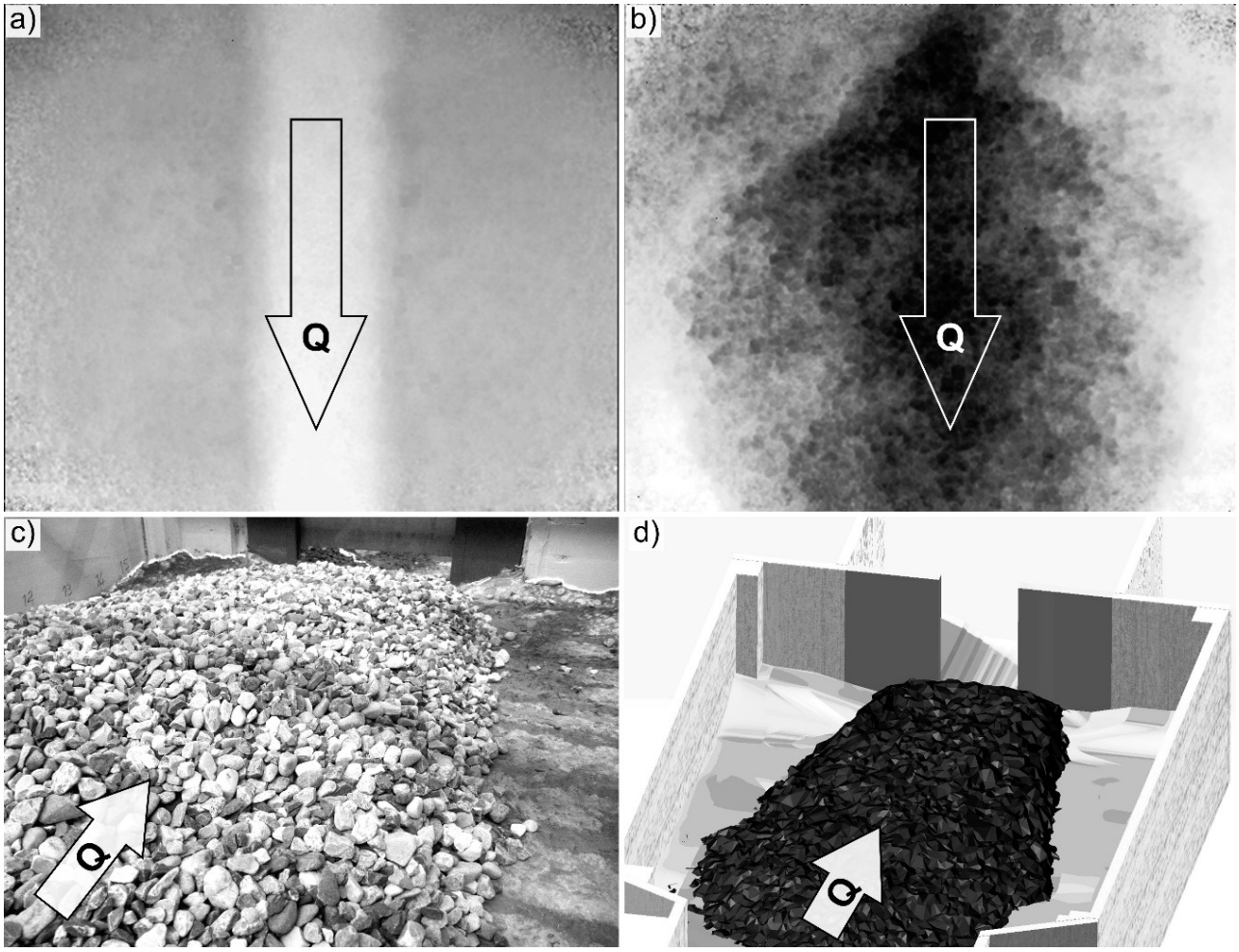

Figure 2: Example of the recording of the deposition area bathymetry with the motion sensing device: (a) a gray-scale picture of the empty deposition area (top-view) and (b) a gray-scale picture of the deposition area with sediment (top-view). A picture from a standard camera of the deposit at the end of the *HyMec.a1 α*-test is shown in (c), with its numerical representation derived from the motion sensing device (d).